FDM Printability of PLA Based-Materials: The Key Role of the Rheological Behavior

buildings

MDPI

Article

Dynamic Structural Identification of a Portion of the Medieval Defensive Walls of Verona, Italy, Through Ambient Vibration Test

Riccardo Mario Azzara [1], Marco Tanganelli [2,*], Francesco Trovatelli [3] and Paolo Venini [4]

[1] Osservatorio Sismologico di Arezzo, Istituto Nazionale di Geofisica e Vulcanologia (INGV), Via F. Redi, n. 13, 52100 Arezzo, Italy; riccardo.azzara@ingv.it
[2] Dipartimento di Architettura (DiDA), Università degli Studi di Firenze, Piazza Brunelleschi n. 6, 50121 Firenze, Italy
[3] Department of Structural, Geotechnical, and Building Engineering (DISEG), Politecnico di Torino, Corso Duca degli Abruzzi 24, 10129 Turin, Italy; francecso.trovatelli@polito.it
[4] Dipartimento di Ingegneria Civile e Architettura, Università di Pavia, Via Adolfo Ferrata, n. 3, 27100 Pavia, Italy; paolo.venini@unipv.it
* Correspondence: marco.tanganelli@unifi.it

Abstract

The study focuses on the results of the analysis of data recorded during Ambient Vibration Tests (AVT) conducted on a portion of the Medieval Walls of Verona (Northern Italy). Seismometric stations were installed both at the top and at the base of the walls, recording the free vibrations of the structure. Spectral analyses provide information about the principal modal frequencies, which are compared with the results obtained through Operational Modal Analysis (OMA) techniques. Numerical models were developed to describe the elastic behavior of the walls and to support the interpretation of the experimentally identified modes. Seismic noise measurements were also performed on the ground to characterize the spectral response of the soil and to estimate the soil–structure interaction. The combined use of AVT data, OMA procedures, and numerical modeling allowed for a robust identification of the fundamental dynamic properties of the walls, highlighting the predominance of out-of-plane modes and the limited dynamic coupling with the underlying soil. The study demonstrates the effectiveness of this non-invasive approach for improving the knowledge of structural assessment, reducing uncertainties in mechanical parameter calibration, and supporting informed conservation, maintenance, and risk-mitigation strategies for historic defensive masonry structures.

Keywords: seismic monitoring; medieval city walls; AVT; OMA; soil-structure interaction

Academic Editors: María Victoria Requena García de la Cruz and Madalena Ponte

Received: 31 December 2025
Revised: 15 February 2026
Accepted: 17 February 2026
Published: 24 February 2026

1. Introduction

The preservation of historic masonry buildings represents a central topic within the field of Structural Engineering. Among linear historical structures, urban defensive walls are a widespread architectural typology in historic centers and form an important part of the cultural heritage. However, probably due to their robust and reassuring appearance and the perception that they have successfully passed the so-called "test of history," insufficient attention is often given to their structural safety [1]. The frequent collapses of sectors of the historic city walls (e.g., Pistoia, Italy, in 2011 and 2020, [2]; Volterra, Italy, 2014 and 2024; San Gimignano, Italy, in 2018) highlight that without planned maintenance these

structures can become vulnerable elements [3], and their sudden collapse may pose hazards to infrastructure and civil security.

Although historical defensive walls are conceptually simple—consisting of a thick wall extending in length—they often present features that complicate their structural behavior. These include variations in cross-section, heterogeneous construction materials and techniques (both in thickness and extension), differences in ground levels on either side, and foundations resting on inclined terrain with variable geotechnical properties. The introduction of reinforcing elements, such as barbicans, or discontinuity elements such as towers or city gates, further interrupts structural continuity and influences the overall response of the wall.

Defensive walls are exposed to multiple vulnerabilities, arising from both environmental and anthropogenic sources. In urban areas, they may experience long-term degradation due to vehicular traffic. Additionally, climate-change-induced phenomena and natural hazards—such as foundation settlement caused by moisture accumulation from heavy rainfall, flooding, or inadequate drainage—can compromise structural stability. Seismic actions represent a critical factor for the local collapse of structural portions or for free-vibrating non-structural elements, such as merlons [4]. Assessing seismic vulnerability requires understanding both the seismic exposure (site and source effects) and the dynamic response of the structure, which depends on geometry, mechanical properties, and preservation state.

In this context, Ambient Vibration Test (AVT) provides a non-invasive diagnostic tool for assessing the dynamic behavior of historical structures [5]. When combined with Operational Modal Analysis (OMA) procedures [6], AVT allows the identification of dynamic properties, such as natural frequencies, mode shapes, and damping ratios. These data, integrated with finite element (FE) models, support the calibration of numerical simulations and the execution of seismic vulnerability assessments.

In the literature, AVT and OMA techniques have been applied to various architectural typologies, including religious buildings such as churches and cathedrals [7–10], slender structures such as towers and bell towers [11–19], building aggregates [20], infrastructural structures such as bridges and aqueducts [21,22], and palaces and monumental buildings [23–25].

Despite these applications, the systematic use of AVT and OMA on historic urban defensive walls remains very limited; a small number of publications can be found in the literature, leaving a significant gap in the state of the art.

Unlike isolated buildings or slender structures, extended defensive walls are linear, heterogeneous, and historically stratified, presenting unique challenges in monitoring and numerical modeling. This paper aims to further contribute to the recognition of the importance of promoting experimental studies on urban walls, in order to develop a knowledge practice that would be preparatory to prevention.

Comprehensive studies of defensive walls should generally adopt an integrated approach [26,27], combining historical research with non-destructive testing and geotechnical investigations to reconstruct construction history, identify past alterations, and characterize materials and foundation soils. These datasets are essential for performing advanced numerical analyses [28], including kinematic analyses according to reference standards [29,30] and FEM simulations capable of reproducing complex phenomena, such as differential settlements and moisture-induced soil weakening under seismic loads [31].

Integrating AVT results with numerical modeling on extended defensive wall systems enables a more accurate characterization of structural dynamic behavior, improves model calibration, reduces uncertainties in mechanical parameter definition, and allows long-term monitoring of dynamic changes due to environmental actions, climate effects, or localized damage.

This study applies seismic monitoring techniques to a portion of the defensive Walls of Verona, Italy, specifically the Magistral Walls located in the hilly area between the breach of Castel S. Pietro and the fort of S. Felice. Constructed during the Scaliger period (1200–1300) and subsequently modified in the Habsburg period (first half of the 1800s), this segment represents a complex case study characterized by diverse masonry textures, geometric variability, and substantial ground remodeling associated with twentieth-century interventions.

The wall portion forms part of a broader project aimed at establishing guidelines for the documentation, conservation, and maintenance of the Magistral Walls of Verona [32], with further details available in [33–38].

More specifically, the objective of the present study is the experimental dynamic identification of a portion of historic defensive walls through Ambient Vibration Tests, articulated into three main research objectives. First, the study aims at the identification of the fundamental modal parameters of continuous masonry curtain walls. Second, it investigates the possible spatial migration of modal frequencies along the walls. Third, the experimental results are preliminarily and qualitatively validated through comparison with a simplified numerical model.

The paper is organized as follows. Section 2 describes the case study and the survey campaign on the Walls and the surrounding terrain; Section 3 presents the results of frequency-domain analyses conducted on both the walls and the soil; Section 4 discusses the OMA results and the comparison with a simplified numerical model; and Section 5 summarizes the conclusions.

2. The Case Study

2.1. Historical and Architectural Framework

The portion of the walls under consideration belongs to the Magistral Walls and is located in the hilly area between the breach of Castel S. Pietro and the fort of S. Felice. Here, the curtain wall corresponds to the Scaliger model of a medieval layout with a facing interspersed with towers and topped with merlons.

Constructed during the Scaliger period (1200–1300) and subsequently modified in the Habsburg period (first half of the 1800s), this segment corresponds to a section of the 'Cammino di Cangrande'. Despite its modest extension of approximately 300 m, it provides a rich and functional case history of masonry texture for experimentation. Scaliger masonry, characterized by its alternation of cobblestone recurrences and brick inserts, is interspersed with portions that feature polygonal masonry from the Austrian period. However, the most substantial alterations to this complex are undoubtedly attributable to the infrastructural transformations and restoration work undertaken between 1938 and 1950, which resulted in the comprehensive remodeling of the entire section of the ground.

The section of the walls investigated was the subject of a project that sought to define guidelines and standardized intervention protocols for implementing specific monitoring, conservation, and maintenance actions of the defensive walls [32].

Detailed information about the historical evolution of the Verona Defensive Walls can be found in [33–38].

The total length of the monitored part of the walls is about 140 m, which was divided into two sections. The first one is about 55 m, and the second one, inclined with respect to the first, is about 85 m long; the two distributions overlap for approximately 25 m in the central part of the section of the walls. Due to the impenetrability of the vegetation, it was not possible to extend the first section up to the bastion of Porta San Felice. The walls follow a slope with an average inclination of about 8/9 degrees. Two masonry bastions are located at both ends of the studied portion, which visually appear to be firmly connected to the walls. The heights of the walls vary according to the ground level, and part of them

act as a retaining wall on the internal side. The difference between the two levels can reach, in some points, up to about 10 m.

2.2. Experimental Activities on the Walls and on the Soil

The free vibration campaign involved the use of equipment from SARA Electronic Instruments, which includes nine three-axis seismometers with eigenfrequencies of 2.0 and 4.5 Hz, coupled to 24-bit Digital Acquisition Systems (DAS). Using a forklift, the sensors were positioned on top of the Walls and connected to the DAS on the ground via a cable (Figure 1). Each device was synchronized through a GPS connection.

Figure 1. Example of a sensor installed on the top of the walls.

The measurements on the two sections of the Walls were carried out on two different days, more or less at the same time, for approximately three hours.

To characterize the elastic properties of the ground, seismic noise measurements were performed on the surrounding terrain on the third day. Figure 2a shows the location of the measurement points on the Walls; Figure 2b shows the distribution of the measurement points on the terrain.

During the first day, the sector between the SW bastion and the point where the Walls bend towards NE was monitored (first sector in Figure 2a), and the following section was monitored on the second day. At the beginning and end of each sector, two seismic stations (in yellow in Figure 2) were installed at the base of the Walls, to be used as a reference on the ground.

The sensor spacing on the Walls was optimized to not exceed 15 m, with the aim of obtaining a good spatial resolution for defining the modal shapes of the structure. The three-axis velocimeters were oriented so that at each point the X-axis corresponded to the longitudinal direction of the Walls (in-plane) and the Y-axis to the transverse direction (out-of-plane), in the direction of the public park (Figure 1). The data, sampled at 100 sps, were recorded for three hours during each experiment. Before proceeding with the analysis, the data were corrected for the instrumental curve.

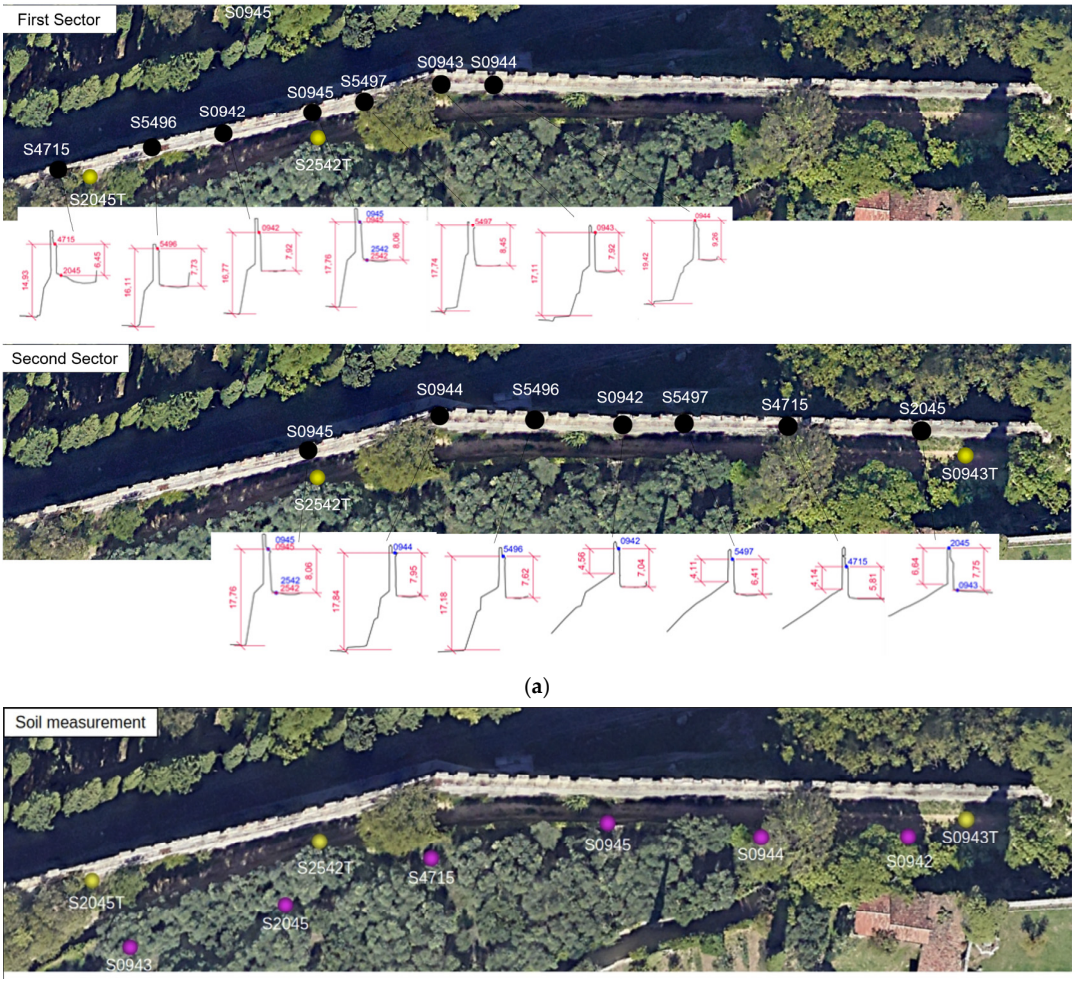

(**a**)

(**b**)

Figure 2. (**a**) Measurement points on the Walls during the two days (black circles); for each point, the corresponding cross-section of the Walls is shown. At the top is shown the first sector monitored during the first day; at the bottom, the second sector. In yellow the seismic stations installed at the base of the Walls during the first and second experiments. (**b**) Map of the seismic stations installed on the ground on the third day of measurements (in magenta); in yellow, those installed at the base of the Walls during the first and second experiments.

3. Frequency Domain Analysis

3.1. Spectral Behavior of the Walls

For each measuring point, the average spectra were estimated as the geometric mean of the FFTs computed for each component of motion over all the two-minute segments (120 s) contained in the total recording. As can be seen from the example in Figure 3, the spectral amplitude associated with the out-of-plane direction (Y) at each measuring point is dominant compared to the other components, with the spectral peaks amplitude ranging from 5 to 20 times greater than those along the in-plane direction (X). Therefore, the analysis was limited to the out-of-plane component (Y).

Figure 4 shows the average FFTs for each measuring point along the first and second sectors of the Walls. The two monitored sectors seem to show, both in spectral amplitude and frequency, a different behavior.

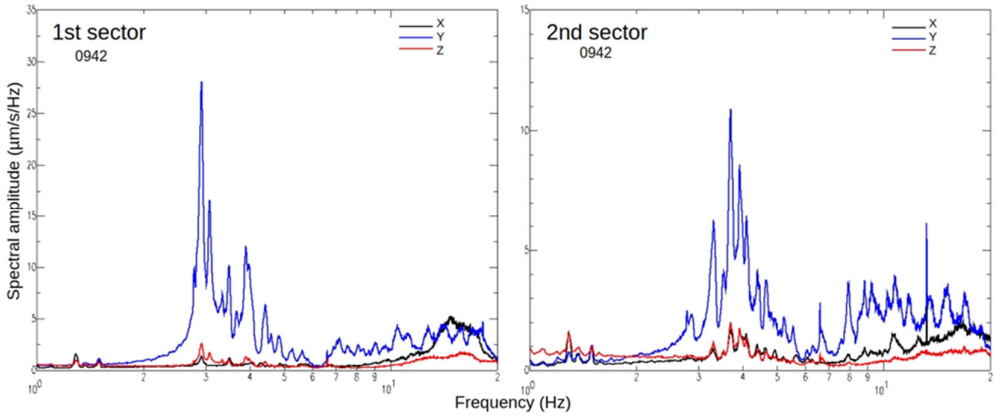

Figure 3. Comparison between the average spectra estimated from the recordings in the first and second experiments. Black, blue, and red curves correspond respectively to X, Y, and Z components.

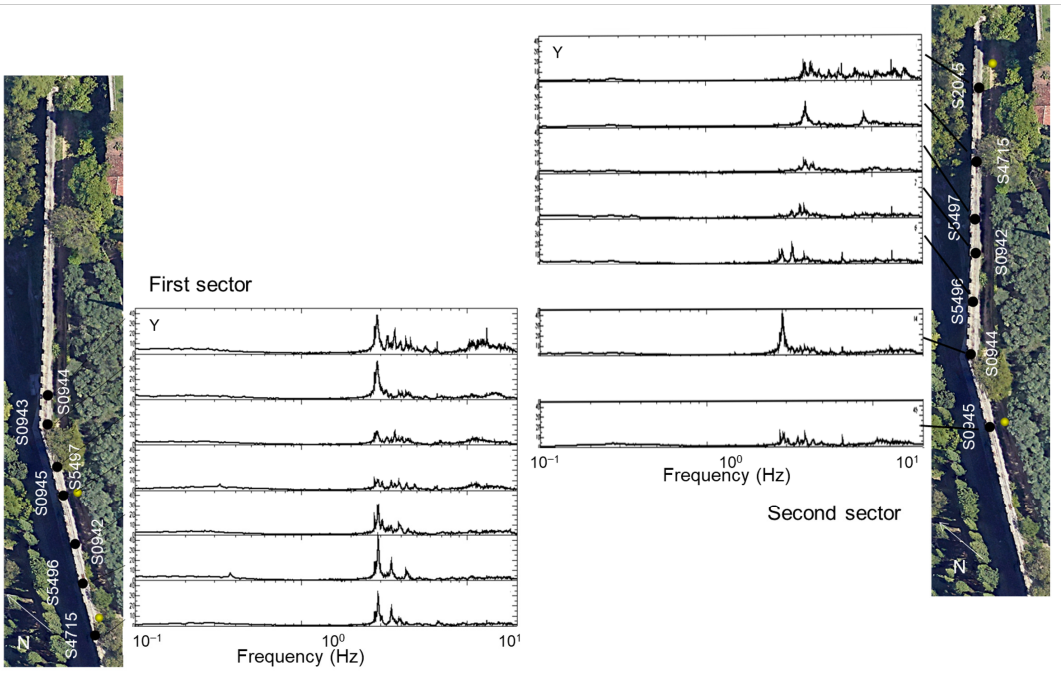

Figure 4. Distribution of the average spectra along the out-of-plane (Y) direction for each monitored point on the first and second sectors of the Walls.

In the first segment, all the monitored points exhibit almost the same spectral behavior. It has to be noticed that in the central part of the profile (stations 0945 and 5497), spectral amplitudes are lower by at least a factor of 3 compared to those of the other points of the sector. This could be due to the possible presence of a node in this area for the modal shape corresponding to the principal frequency of the segment. Despite this aspect, in this first section, the FFTs show spectral peaks centered practically on the same frequency, around 2.92 Hz. Only in the last two points of the alignment (0943–0944), positioned beyond the fold of the Walls, a slight reduction in the peak frequency of the spectrum is recorded, which is centered around 2.88 Hz.

The situation is quite different in the sector monitored during the second day (Figure 2a, bottom). A spatial variation in the frequency associated with the first spectral mode is evident, gradually increasing from 2.8 Hz to 4 Hz. Probably due to the changing orientation corner at the beginning of the alignment and to the presence of the bastion at the end, the central part of the sector exhibits more stability than the extremes, showing spectral amplitudes that are significantly less than of those at its end. In Figure 4, the first two

FFTs from the bottom correspond to the measurement points that during the second test occupied the same positions as the first, so as to guarantee continuity of the recordings.

In order to better highlight the gradual variation in the modal frequency along the stations of the second sector, in Figure 5, an enlarged detail of Figure 4 over the frequency range 1.5–5.5 Hz is shown. Looking at Figure 5, it seems plausible to hypothesize that as one approaches the most rigid part of the structure represented by the bastion at the end of the section, each of the monitored portions in the second segment is sensitive to the effect produced by higher-order harmonics.

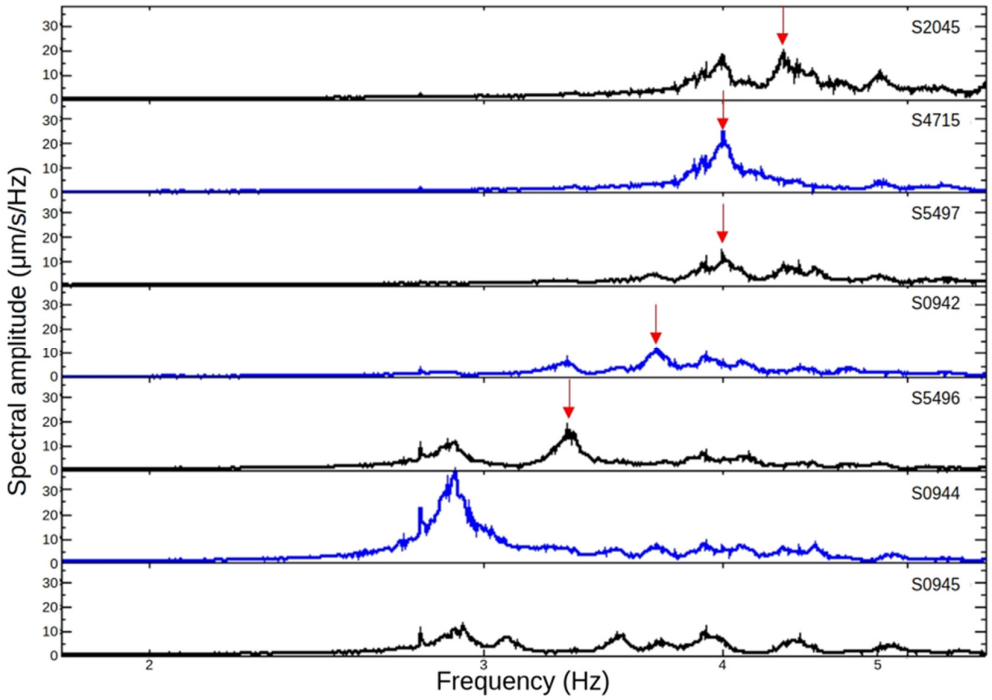

Figure 5. Linear spectral profile along the NE-oriented sector, monitored during the second day of measurements. The red arrows correspond to the peaks that could be considered representative of the main mode of each segment considered.

Moreover, the migration towards high frequencies of the main mode estimated for each measurement point along the second segment could be related to the effect produced by the tower placed at the end of the segment, which should constitute an element that, by stiffening the structure, tends to lock the out-of-plane motion of the Walls.

Comparing the spectra calculated on the fixed-point recordings shows how accurately and over which frequency band they can be considered points of continuity.

Figure 6 shows the stability of the estimated spectra at the two fixed measurement points during the two experiments. Despite some moderate low-frequency variations (<1.0 Hz), particularly evident on the vertical component, it can be observed that the signals from the stations that monitored the same points at different times, show substantially overlapping trends over a frequency band that, after applying the instrumental correction, covers almost the entire engineering bandwidth of interest, at least from 0.3 Hz up to 20 Hz, which in the case of the horizontal components can be extended down to 0.1 Hz. For this reason, these records were used as alignment points to connect measurements collected at different times on the two sectors of the Walls in the OMA procedures.

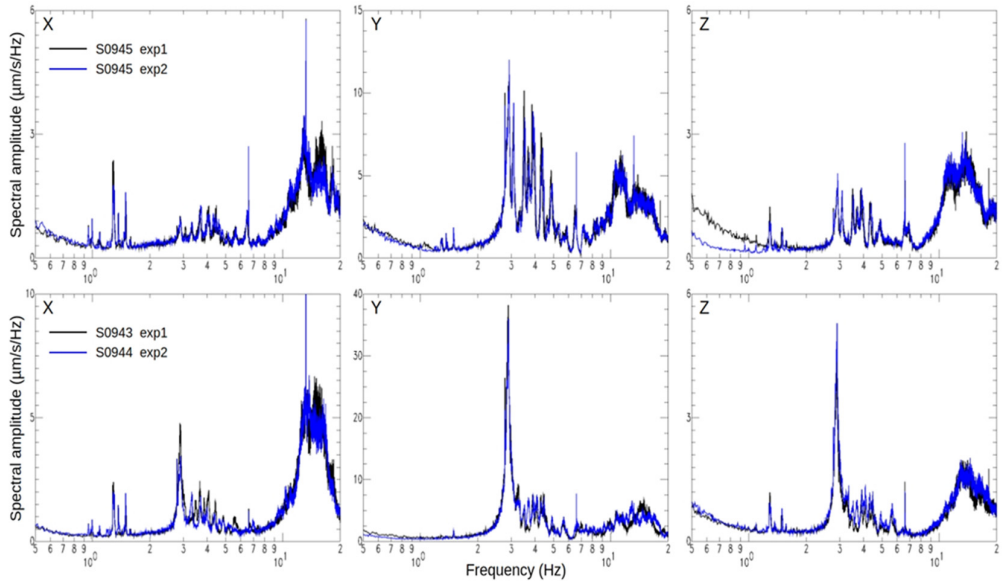

Figure 6. Comparison between the average spectra recorded by the seismic stations located at the same point during the two experiments.

In order to complete the spectral analysis, an estimate of the empirical transfer function of the Walls was obtained using the Standard Spectral Ratio (SSR) technique. The SSR technique consists of computing the spectral ratio between the seismic station on the Walls and a synchronized reference station installed on the ground, for each motion component. Taking advantage of the presence of the two stations installed on the ground in each segment (in yellow in Figure 2a,b), the SSRs were estimated between the wall-mounted seismic stations and the closest ground station for each measurement point.

Figure 7 illustrates the SSRs calculated for each monitoring point along the out-of-plane direction. These spectral ratios closely align with findings from the spectral analysis.

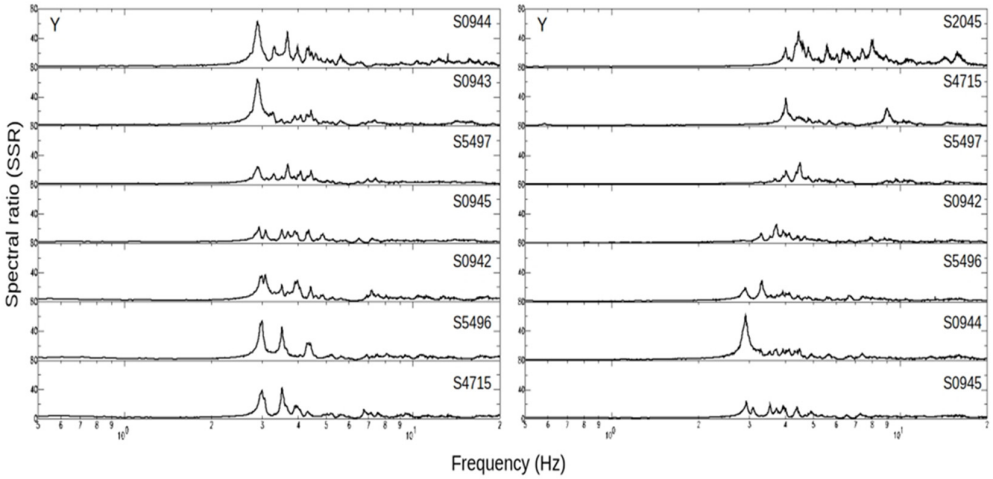

Figure 7. Estimation of the empirical transfer function (SSR) along the out-of-plane direction (Y) for the two monitored sections of the walls; the left panel is the first section, and the right one is relative to the second section.

In the first section of the Walls, a predominant modal frequency around 2.88 Hz is observed, with slight variations along the section. Variations in the amplification factor around this primary modal frequency indicate a central segment less prone to amplifying ground signals, while the initial and final segments show amplification that can reach a factor of about 70. In the second section, the spatial migration of each section's character-

istic frequency is confirmed, with noticeably lower amplification factors compared to the preceding section.

The first two curves from the bottom in the panel relative to the second section correspond to recordings taken at the same points on the first experiment. The amplification values estimated in the SSR at these points over the two recording days are comparable, suggesting that results obtained on different days at different points can be reliably compared and that it is unlikely that the differences in responses between the two sections could result from different solicitations. In order to confirm this observation, it is possible to compare the temporal trends and the spectra of the recordings taken on different days at the same measurement point at the base of the walls (Figure 6).

The empirical transfer functions in Figure 7 show very similar trends to the spectral distribution (Figure 4). To understand the relationship between the Wall and the surrounding terrain, the average spectra calculated on synchronized recordings from seismic stations installed at the top and on the ground were compared (Figure 8).

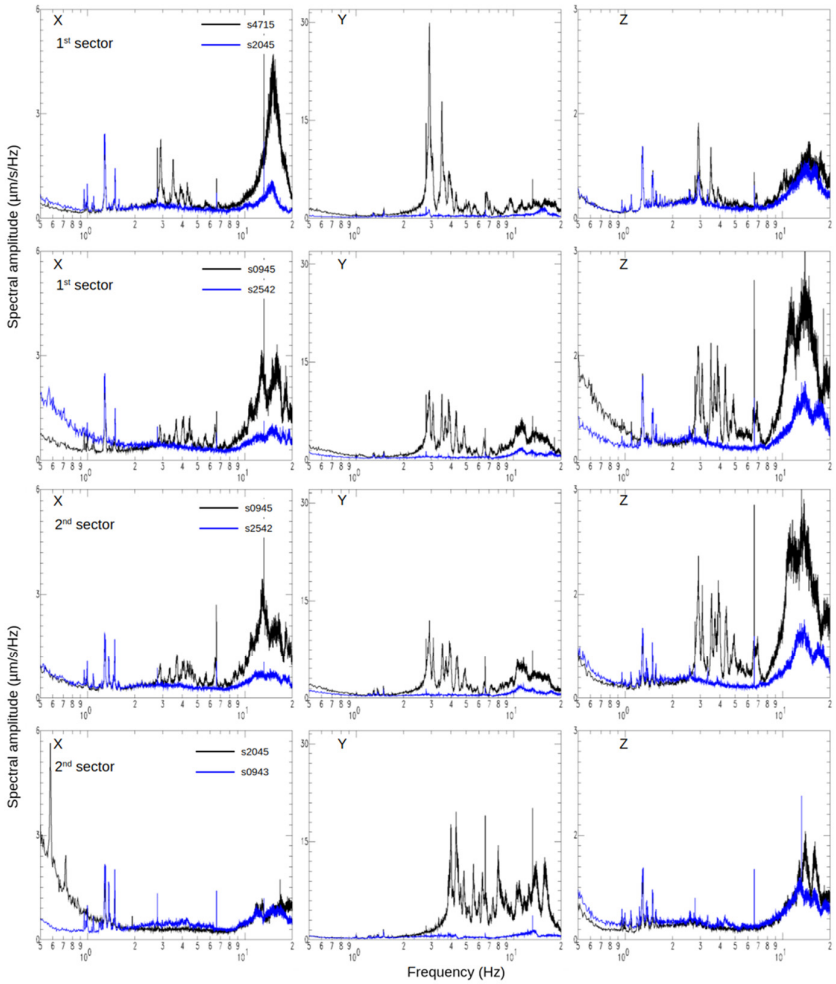

Figure 8. Comparison between the average spectra computed on the data recorded by the stations at the top of the Walls (black curves) and the corresponding recordings performed on the ground (blue curves) during the two experiments.

As can be observed, the ground-averaged spectra show no spectral contribution due to oscillation of the Walls in the frequency band where their modes appear to dominate the spectrum. This is true not only for the out-of-plane component (Y), but also for the other components, despite the former showing an amplitude almost five times greater than the others.

3.2. Spectral Characterization of the Soil

Simultaneously with the measurements on the Walls, seismic ambient noise was recorded on the ground. The position of the seismic station installed at the base of the Walls is depicted in yellow in Figure 2a,b.

After the experiment on the Walls, a third experiment was performed on the ground (Figure 2b): six 2.0 Hz seismometers were installed along a linear profile parallel to the Walls, along the path that runs alongside them at a distance of approximately four meters, oriented in the same direction as the stations installed on the Walls.

In order to estimate the stability of the signal recorded at three different times, the measurements taken in this third experiment were compared with those taken on the ground during the monitoring of the Walls. Figure 9 is the comparison between the average spectra computed from the recordings of the linear transect (black curves) and the measurements at the ground on the first and second experiments, blue and red, respectively.

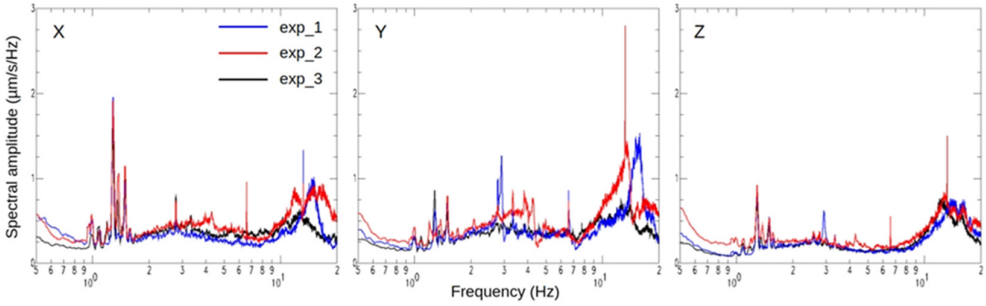

Figure 9. Comparison between the average spectra obtained from the recording of one of the stations installed on soil in the third experiment (black) and one of the seismic stations installed at the base of the Walls during the first (blue) and second (red) experiments.

From Figure 9, it is evident that the spectral trends are coherent, at least up to about 10 Hz at all points, regardless of the position and time of monitoring, confirming a clear homogeneity of the terrain surrounding the Walls.

In order to characterize the spectral behavior of the soil, according to Nakamura [39], spectral ratios (HVSR) between the horizontal and vertical components were calculated from the recorded waveforms to estimate the resonance frequency of the site (Figure 10).

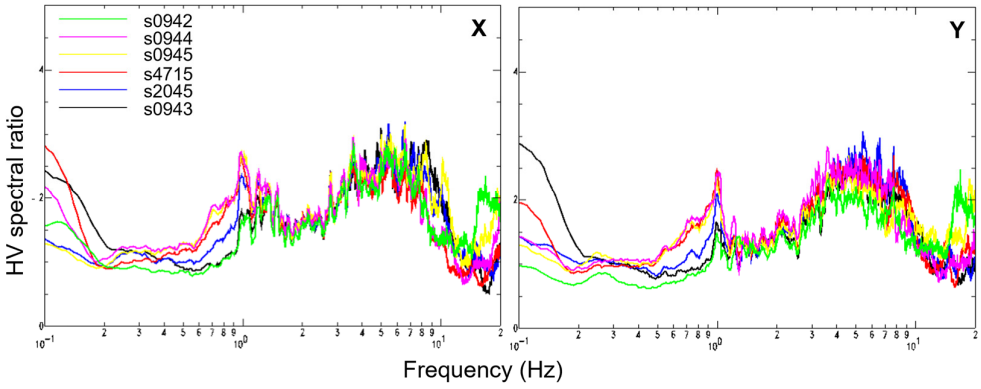

Figure 10. Spectral ratios HVSR computed for each seismic recording along the linear profile on the soil, respectively; on the left are the ratios of the component X, on the right are those of the component Y.

The choice to show the ratio of the single X/V and Y/V components instead of the geometric mean between them, HV, following the guidelines of the SESAME Project [40], arises from the intent to highlight that the two horizontal directions produce the same ratio, demonstrating that there is no directionality in the ground and, despite the great

prevalence of the out-of-plane motion of the Walls, this does not influence the spectral behavior of the surrounding soil.

The excellent consistency of the spectral ratios for all seismic stations and on both components of the motion led to the hypothesis that the ground along the monitored part of the Walls has a strong homogeneity. In both directions, there are two large spectral peaks. The first is centered on a frequency of about 1 Hz and has a spectral amplitude of about 1 Hz; the second, higher than the previous one, is centered around 5.5 Hz with a spectral extension over about 6 Hz. Following the requirements of the SESAME project guidelines [41], taking into account the amplitude of both the spectral peaks does not exceed a factor 3 and the large spectral band of the peaks, it is possible to say that no marked effects of surface amplification due to sharp changes in the contrast of acoustic impedance between the surface layer and the geologic bedrock could be hypothesized, suggesting that area surrounding the Walls seems not to exhibit clear effect of surface amplification.

In this view, according to the maps attached to the Level 1 Seismic Microzonation report published in April 2017 [41] and available on the website of the municipality of Verona, the monitored sector can be placed within a homogeneous area corresponding to the geologic substrate class described as "soft rocks with a predominant cohesion and the composition of limestone". Despite the fact that none of the microtremor measurements executed during the microzonation appear to have been carried out in the vicinity of the monitored area, the frequency peaks obtained from the HV analysis are, however, consistent with the microzonation results.

4. Operational Modal Analysis and Numerical Modeling

The modal analysis on the recordings was conducted by using the commercial Artemis Modal Pro Software. The first of the two setups on which the analysis was performed concerns the portion of the walls located in the first section and in a part of the second (Figure 2a); the second one refers to the second sector of the Walls (Figure 2a). For each point, a one-hour recording was considered. Figure 11a shows the simplified geometry of the model used for the OMA, developed in the Artemis environment; the points of alignment between the two setups are depicted in blue (points 4 and 27).

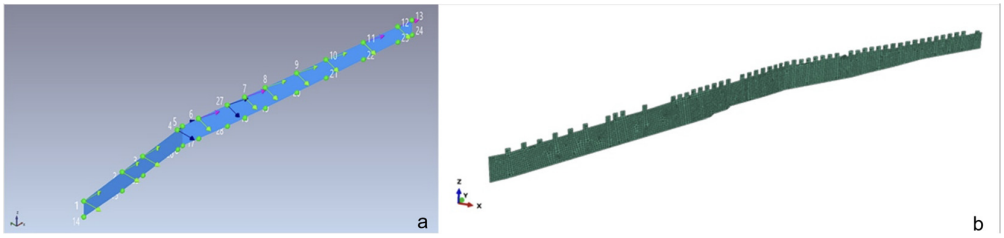

Figure 11. (**a**) Reference geometry of the complete model of the two setups; note that the points 5, 13, and all the lower ones are elements fixed for purely representative purposes; (**b**) the numerical model.

The following analysis was performed considering the two sectors together in order to obtain a complete overview of the average spectrum for the entire monitored portion of the walls. The vertical component was excluded from the analysis. Figure 12 shows the average spectrum computed through the Frequency Domain Decomposition (FDD) method. In the average spectrum of Figure 12, the peak at 2.88 Hz stands out, to which the modal shape corresponds; a frequency very close to that experimentally estimated for the first section of the walls.

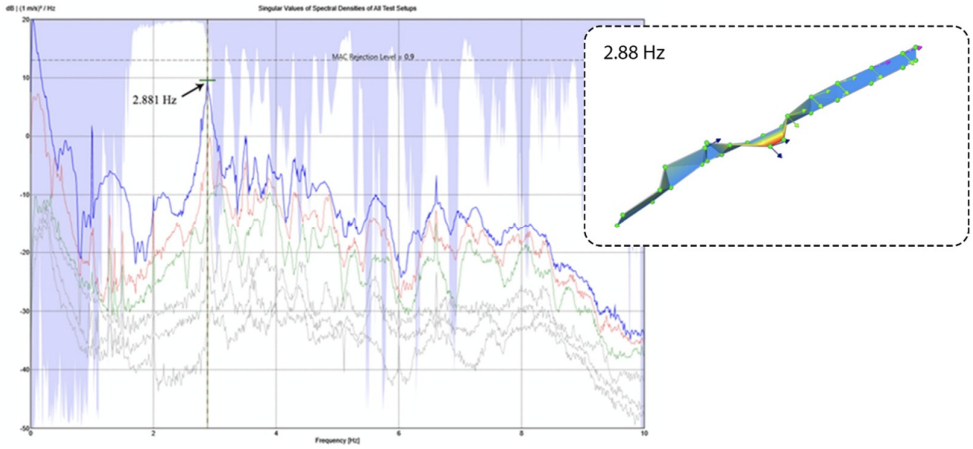

Figure 12. Average spectrum (FDD, in blue). The green dotted vertical line identifies the peak corresponding to the fundamental frequency, estimated at 2.88 Hz. The modal shape corresponding to the 2.88 Hz, the first modal frequency, is shown in the insert.

The variations in the dynamic characteristics of the structure in its main parts mutually affect the modal shapes of the higher modes, making it difficult to interpret the results in the high-frequency range, in which the spectral peaks are not as clear as those associated with the first mode.

For this reason, an additional analysis was conducted, taking into account only the last monitoring point of the first section of the Walls and all the points of the second segment. Figure 13 shows the results for this additional model.

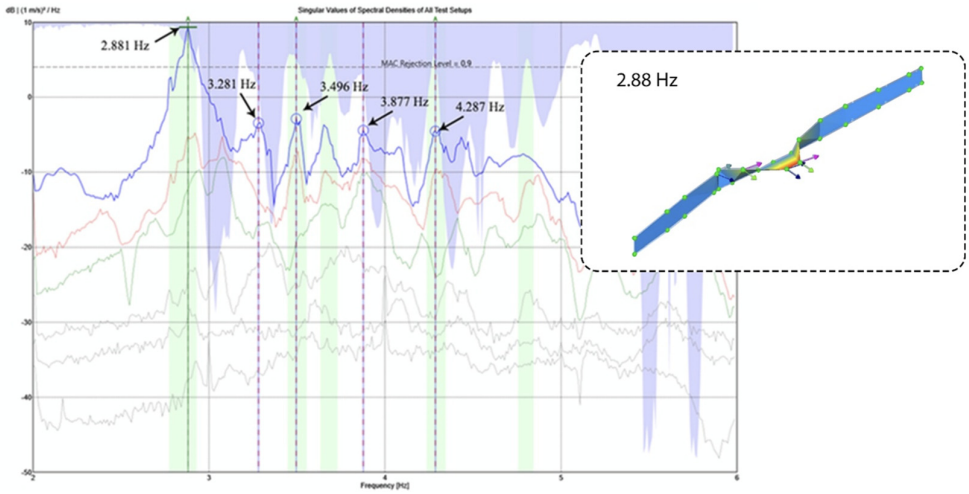

Figure 13. Average spectrum for the model of the second sector of the Walls; the average spectrum (FDD), highlighted in green, is the 2.88 Hz main frequency. The spectral domain ranges from 2 to 6 Hz. The insert corresponds to the mode shape associated with the main frequency.

Also in this case, the 2.88 Hz mode clearly emerges, relating to the initial segment of the second sector, characterized by an out-of-plane motion and corresponding to the highest area of the Walls, as can be recognized from the associated modal shape.

Considering the complexity of the case study, the main goal of the analysis was to estimate at least the frequency and the modal shape for the fundamental mode. As can be deduced from Figures 12 and 13, it is not possible to clearly identify the higher modes of the structure. A useful approach in this context could be to use a numerical model capable of providing at least a qualitative view of the deformation associated with the higher modes of the Walls.

The proposed numerical model (Figure 11b), developed with the commercial FEM software Abaqus [42], is characterized by shell elements with a constant thickness of one meter of homogeneous and continuous material (Elastic modulus = 4500 MPa, specific weight = 1800 kg/m^3, Poisson coefficient = 0.28), fixed at the base. Although the elastic modulus, chosen to fit the frequency of the first mode, seems high, it is common in the literature that the values used in real cases can result in higher values than those described in the international standards.

The numerical model was defined over the entire extension of the walls portion subjected to monitoring, but, in order to facilitate a direct comparison with the OMA results, constraints were imposed on the translations and rotations in every direction for the nodes of the first section of the walls (not studied), focusing on the results of the modal analysis obtained for the second sector of the walls.

Figure 14 shows the first five numerical modes of the structure, highlighting a flexional sinusoidal out-of-plane shape in ascending order (mode 1, simple bending; mode 2, double bending; mode 3, triple bending, etc.). These are compared with experimental mode shapes obtained experimentally through the OMA method.

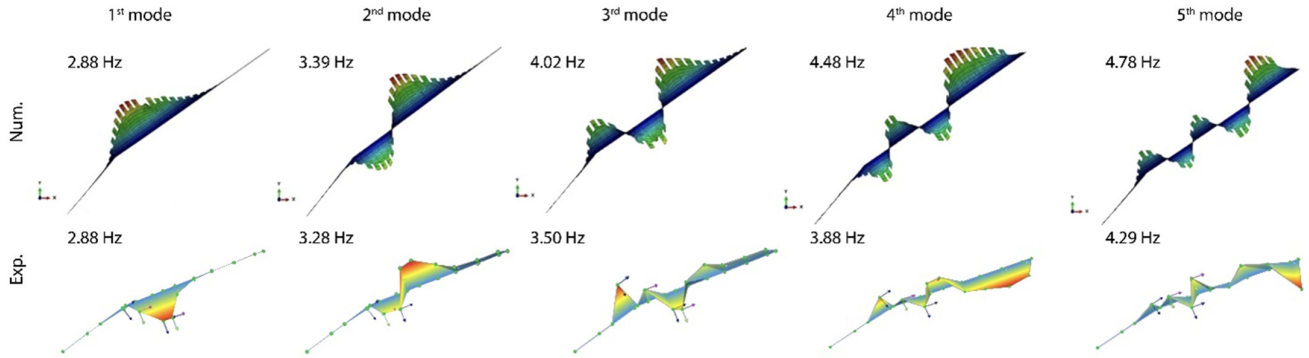

Figure 14. The first five numerical and experimental modal shapes were obtained numerically and through the Operational Modal Analysis method.

The frequency range of the first five numerical modes extends from about 2.8 to 5 Hz, in good agreement with that previously obtained from OMA and with the experimental estimates (Figure 5). It is interesting to notice that, despite the simplicity of the model, the numerical mode shapes exhibit quite good agreement with those estimated by OMA.

5. Discussion and Conclusions

This study represents one of the first contributions to the dynamic identification of a historical wall segment based on in situ monitoring and Operational Modal Analysis. The object of the paper is aimed at characterizing the dynamic response of the investigated wall portions and to provide preliminary, experimentally based information to support subsequent structural analyses. In particular, the results could constitute a basis for the identification of the main collapse mechanisms associated with the identified modal shapes and for the calibration and constraint of a global finite element model, to be adopted in future structural assessment and vulnerability evaluations.

The results of the analyses allow us to make some considerations about the dynamic behavior of the monitored segments:

- The measurements show that the predominant oscillation is transversely oriented to the Walls' axis (Y, out-of-plane direction). The Walls exhibit a significant response only within the frequency range from 2 Hz to 10 Hz. Within this range, similar spectral patterns are observed across all three motion directions, with out-of-plane motion remaining predominant.

- The results from spectral analysis would report that the two sectors of the Walls show different behavior. In the spectral range of 2.0–10.0 Hz, which includes the primary modal frequencies, distinct behavioral modes are discernible in the two monitored sections. In the section monitored during the initial experiment, from the beginning of the measurements to the point where the axis of the Walls bends by about 15°, there is substantial spectral uniformity across different measurement points, identifying a common primary modal frequency around 2.88 Hz in all recordings and motion directions, although the spectral amplitude is reduced in the central part. In the second section, the spectral characteristics of out-of-plane motion are identifiable in the other motion components. The modal frequency estimated in each measuring point changes in a range from 2.8 Hz to 4 Hz, from the points corresponding to the first day of measurements towards the end of the deployment. The variation in the frequency could be linked to the variation in the height of the Walls. The cross sections show that, while in the first section the height of the Walls does not change significantly, in the second sector it exhibits greater variability, gradually decreasing from 8 m to less than 6 m.
- The results of applying the OMA technique allowed us to identify the main modal frequency in the transverse direction. In particular, the use of OMA proved particularly effective in capturing the gradual variation of modal frequencies associated with the recognition of higher-order modal frequencies, when applied to small portions with similar physical, mechanical, and geometric characteristics.
- The elastic parameters used to create a numerical model fitting the experimental modal frequencies are higher than those required by the regulations. This applies in particular to the elastic modulus.
- The microtremor measurements show that the ground has a homogeneous behavior along the whole measuring area. The amplitude of the HV spectral ratio peaks shall not exceed the value 3, indicating that there is no strong impedance contrast between the surface layers and the rigid substrate.
- Comparison with simultaneous ground-level measurements shows significant correspondence at both low (0.5–2.0 Hz) and high frequencies (10–20 Hz). However, in the frequency band 2.0–10.0 Hz, the spectra of ground-level stations appear to indicate an almost complete decoupling between the walls and the ground.
- In the 2.0–20.0 Hz band, spectral lines are present on all measurement components on the Walls and on the ground, likely originating from oscillation sources within the study area.

Author Contributions: Conceptualization, R.M.A., M.T., F.T. and P.V.; methodology, R.M.A., M.T. and F.T.; software, R.M.A. and F.T.; validation, R.M.A. and F.T.; formal analysis, R.M.A. and F.T.; investigation, R.M.A. and F.T.; data curation, R.M.A. and F.T.; writing—original draft preparation, R.M.A. and F.T.; writing—review and editing, R.M.A., M.T., F.T. and P.V.; visualization, R.M.A., M.T. and F.T.; supervision, R.M.A. and M.T.; project administration, P.V. All authors have read and agreed to the published version of the manuscript.

Funding: This research was supported by funding from the Municipality of Verona within the framework of projects on analysis and strengthening protocols for the city walls between Castel San Pietro and Castel San Felice.

Data Availability Statement: The data that support the findings of this study are available from the corresponding author, M.T., upon reasonable request.

Acknowledgments: Special thanks go to the Municipality of Verona for the logistical support for the installation of the instrumentation at the top of the Walls. Thanks go to the research group coordinated by S. Parrinello for involving us in the study of the Defensive Walls of Verona. Verdiana

Leto, Fabiana Barone, and Maria Rosaria Palo edited the first draft of the English version during their university internship at the Seismological Observatory of Arezzo as part of the degree course in Languages for Business Communication at the University of Siena.

Conflicts of Interest: The authors declare no conflicts of interest.

References

1. De Falco, A. Valutazione dello stato di sicurezza delle mura urbane. In *LE MURA URBANE CROLLANO. Conservazione e Manutenzione Programmata della Cinta Muraria dei Centri Storici*; Pisa University Press: Pisa, Italy, 2018; pp. 73–86, ISBN 978-88-3339-175-5. (In Italian)
2. Andreini, M.; De Falco, A.; Giresini, L.; Sassu, M. Collapse of the Historic City Walls of Pistoia (Italy): Causes and Possible Interventions. *Appl. Mech. Mater.* **2013**, *351–352*, 1389–1392. [CrossRef]
3. Di Sivo, M.; Ladiana, D. (Eds.) *LE MURA URBANE CROLLANO. Conservazione e Manutenzione Programmata della Cinta Muraria dei Centri Storici*; Pisa University Press: Pisa, Italy, 2019, ISBN 978-88-3339-175-5.
4. Ferretti, D.; Coïsson, E.; Lenticchia, E. Seismic Damage on Merlons in Masonry Fortified Buildings: A Parametric Analysis for Overturning Mechanism. *Eng. Struct.* **2018**, *177*, 117–132. [CrossRef]
5. De Stefano, A.; Matta, E.; Clemente, P. Structural Health Monitoring of Historical Heritage in Italy: Some Relevant Experiences. *J. Civ. Struct. Health Monit.* **2016**, *6*, 83–106. [CrossRef]
6. Brincker, R.; Ventura, C.E. *Introduction to Operational Modal Analysis*, 1st ed.; John Wiley & Sons, Ltd.: Hoboken, NJ, USA, 2015; 372p. [CrossRef]
7. Gentile, C.; Ruccolo, A.; Canali, F. Continuous monitoring of the Milan Cathedral: Dynamic characteristics vibration-based, S.H.M. *J. Civ. Struct. Health Monit.* **2019**, *9*, 671–688. [CrossRef]
8. Di Giulio, G.; Vassallo, M.; Boscato, G.; Dal Cin, A.; Russo, S. Seismic monitoring by piezoelectric accelerometers of a damaged historical monument in downtown L'Aquila. *Ann. Geophys* **2014**, *57*, 6. [CrossRef]
9. Faleschini, F.; Toska, K.; Feltrin, G.; Zanini, M.A.; Andreose, F.; Hofer, L.; Pellegrino, C.; De Domenico, D.; Ricciardi, G. Structural Health Monitoring of a Historical Church in Italy. In *Proceedings of the 10th International Operational Modal Analysis Conference (IOMAC 2024)*; Rainieri, C., Gentile, C., López, M.A., Eds.; Lecture Notes in Civil Engineering; Springer: Cham, Switzerland, 2024; Volume 154, pp. 176–183. [CrossRef]
10. Masciotta, M.G.; Ramos, L.F.; Lourenco, P.B. The importance of structural monitoring as a diagnosis and control tool in the restoration process of heritage structures: A case study in Portugal. *J. Cult. Herit.* **2017**, *17*, 36–47. [CrossRef]
11. Gentile, C.; Guidobaldi, M.; Saisi, A. One-year dynamic monitoring of a historic tower: Damage detection under changing environment. *Meccanica* **2016**, *51*, 2873–2889. [CrossRef]
12. Garcia-Macias, E.; Ubertini, F. Seismic interferometry for earthquake-induced damage identification in historic masonry towers. *Mech. Syst. Signal Process.* **2019**, *132*, 380–404. [CrossRef]
13. Baraccani, S.; Azzara, R.M.; Palermo, M.; Gasparini, G.; Trombetti, T. Long-term seismometric monitoring of the Two Towers of Bologna (Italy): Modal frequencies identification and effects due to traffic induced vibrations. *Front. Built Environ.* **2020**, *6*, 85. [CrossRef]
14. Azzara, R.M.; De Roeck, G.; Girardi, M.; Padovani, C.; Pellegrini, D.; Reynders, E. The influence of environmental parameters on the dynamic behaviour of the San Frediano bell tower in Lucca. *Eng. Struct.* **2018**, *156*, 175–187. [CrossRef]
15. Azzara, R.M.; Girardi, M.; Iafolla, V.; Padovani, C.; Pellegrini, D. Long-term dynamic monitoring of medieval masonry towers. *Front. Built Environ.* **2020**, *6*, 15. [CrossRef]
16. Barsocchi, P.; Bartoli, G.; Betti, M.; Girardi, M.; Mammolito, S.; Pellegrini, D.; Zini, G. Wireless sensor networks for continuous structural health monitoring of historic masonry towers. *Int. J. Archit. Herit.* **2021**, *15*, 22–44. [CrossRef]
17. Azzara, R.M.; Girardi, M.; Padovani, C.; Pellegrini, D. Dynamic behaviour of the carillon tower in Castel San Pietro Terme, Italy. *Struct. Control Health Monit.* **2023**, *2023*, 1045234. [CrossRef]
18. Romero-Sanchez, E.; Morales-Esteban, A.; Bento, R.; Navarro-Casas, J. Numerical modelling for the seismic assessment of complex masonry heritage buildings: The case study of the Giralda tower. *Bull. Earthq. Eng.* **2023**, *21*, 4669–4701. [CrossRef]
19. Azzara, R.M.; Tanganelli, M.; Trovatelli, F.; Vettori, N. Results from the seismometric continuous monitoring of an ancient bell tower: The Arnolfo Tower, Palazzo Della Signoria, Florence, Italy. In *Structural Analysis of Historical Constructions. SAHC 2023*; Endo, Y., Hanazato, T., Eds.; RILEM Book Series; Springer Science and Business Media B.V.: Berlin/Heidelberg, Germany, 2024; Volume 47, pp. 165–178. [CrossRef]
20. Boscato, G.; Baldelli, J.; Baraldi, D.; Brito De Carvalho Bello, C.; Cecchi, A. Experimental and Numerical Procedure for Vulnerability Assessment of Historical Masonry Building Aggregates. *Int. J. Mason. Res. Innov.* **2024**, *9*, 15–41. [CrossRef]

21. Chisari, C.; Zizi, M.; De Matteis, G. Operational Modal Analysis and Structural Identification of a Masonry Arch Bridge. In *Proceedings of the 10th International Operational Modal Analysis Conference, IOMAC 2024*; Rainieri, C., Carmelo, G., Aenlle López, M., Eds.; Lecture Notes in Civil Engineering; Springer Nature: Cham, Switzerland, 2024; Volume 514, pp. 147–154. [CrossRef]
22. Borlenghi, P.; Saisi, A.; Gentile, C. Vibration monitoring of masonry bridges to assess damage under changing temperature. *Dev. Built Environ.* **2024**, *20*, 100555. [CrossRef]
23. Cattari, S.; Sivori, D.; Alfano, S.; Ierimonti, L.; Cavalagli, N.; Venanzi, I.; Ubertini, F. Calibration of numerical models to support SHM: The Consoli Palace of Gubbio, Italy. In Proceedings of the 8th International Conference on Computational Methods in Structural Dynamics and Earthquake Engineering, COMPDYN2021, Athens, Greece, 28–30 June 2021; pp. 3778–3794. [CrossRef]
24. Clementi, F.; Pierdicca, A.; Formisano, A.; Catinari, F.; Lenci, S. Numerical Model Upgrading of a Historical Masonry Building Damaged during the 2016 Italian Earthquakes: The Case Study of the Podestà Palace in Montelupone (Italy). *J. Civ. Struct. Health Monit.* **2017**, *7*, 703–717. [CrossRef]
25. Pierdicca, A.; Clementi, F.; Isidori, D.; Concettoni, E.; Cristalli, C.; Lenci, S. Numerical Model Upgrading of a Historical Masonry Palace Monitored with a Wireless Sensor Network. *Int. J.* Mason. Res. Innov. **2016**, *1*, 74. [CrossRef]
26. Furini, A.; Paternò, M.; Pellegrinelli, A.; Russo, P. Integrated Measurement Techniques for the Monitoring of the Ancient Walls of Ferrara. In *Built Heritage: Monitoring Conservation Management*; Toniolo, L., Boriani, M., Guidi, G., Eds.; Research for Development; Springer International Publishing: Cham, Switzerland, 2015; pp. 155–164. [CrossRef]
27. Giuliani, F.; Gaglio, F.; Martino, M.; De Falco, A. A HBIM Pipeline for the Conservation of Large-Scale Architectural Heritage: The City Walls of Pisa. *Herit. Sci.* **2024**, *12*, 35. [CrossRef]
28. Papadopoulos, K.A. Seismic Stability Assessment of an Ancient Dry Stone Defensive Wall. *Bull. Earthq. Eng.* **2021**, *19*, 463–482. [CrossRef]
29. Cima, V.; Grande, E.; Lirer, S. Proposal for an expeditious seismic vulnerability evaluation of the Italian medieval defensive walls. *Bull. Earthq. Eng.* **2024**, *22*, 5147–5171. [CrossRef]
30. Grande, E.; Lirer, S.; Conte, G.; Nostrali, D.; Milani, G. Analysis of the Seismic Safety Condition of the Defensive Walls of Cittadella. In *Geotechnical Engineering for the Preservation of Monuments and Historic Sites III*, 1st ed.; Lancellotta, R., Viggiani, C., Flora, A., De Silva, F., Mele, L., Eds.; CRC Press: London, UK, 2022; pp. 735–743. [CrossRef]
31. Concu, G.; Deligia, M.; Sassu, M. Seismic Analysis of Historical Urban Walls: Application to the Volterra Case Study. *Infrastructures* **2023**, *8*, 18. [CrossRef]
32. Parrinello, S.; Minutoli, G.; Dell'Amico, A. Dal rilievo digitale al progetto di restauro, linee guida per la conservazione di un tratto di cinta magistrale a Verona. In *Restauro Archeologico*; Firenze University Press: Firenze, Italy, 2023; pp. 200–210.
33. Parrinello, S.; De Marco, R.; Doria, E. Analysis definition of intervention strategies for the conservation of the boundary walls in Verona. In *Defensive Architecture of the Mediterranean*; Bevilacqua, M.G., Ulivieri, D., Eds.; Pisa University Press: Pisa, Italy, 2023; Volume XV, pp. 1113–1121.
34. Picchio, F.; Pettineo, A. Digitalizzare ricostruire e fruire il Castello di Montorio un tassello nella definizione della rotta culturale dei castelli scaligeri. In *Defensive Architecture of the Mediterranean*; Bevilacqua, M.G., Ulivieri, D., Eds.; Pisa University Press: Pisa, Italy, 2023; Volume XV, pp. 1123–1130.
35. Dell'Amico, A. The Walled city of Verona. Integrated survey systems for the enhancement and promotion of Verona's city Walls. *Int. Arch. Photogramm. Remote Sens. Spat. Inf. Sci.* **2023**, *XLVIII-M-2-2023*, 481–489. [CrossRef]
36. Parrinello, S.; Becherini, P. La documentazione delle mura di Verona. Rilievo, analisi e schedatura delle fortificazioni veronesi. In *Defensive Architecture of the Mediterranean, Proceedings of International Conference on Modern Age Fortification of the Mediterranean Coast, FORTMED, Torino, Italy, 18–20 October 2018*; Marotta, A., Spallone, R., Eds.; Politecnico di Torino: Torino, Italy, 2018; Volume 9, pp. 1075–1082.
37. Parrinello, S.; De Marco, R. Experiences of digital survey data applied for the involvement of societal smart-users in cultural heritage awareness. In *Handbook of Research on Implementing Digital Reality Interactive Technologies to Achieve Society 50*; Ugliotti, F.M., Osello, A., Eds.; Advances in Human and Social Aspects of Technology Book Series; IGI Global Scientific Publishing: Hershey, PA, USA, 2022; pp. 344–386. [CrossRef]
38. Parrinello, S.; Porcheddu, G. Documentation Procedures for Rescue Archaeology Through Information Systems 3D Databases. In *Beyond Digital Representation Digital Innovations in Architecture*; Giordano, A., Russo, M., Spallone, R., Eds.; Engineering and Construction; Springer: Cham, Switzerland, 2024. [CrossRef]
39. Nakamura, Y. A method for dynamic characteristics estimation of subsurface using microtremor on the ground surface. *Q. Rep. RTRI* **1989**, *30*, 25–33.
40. Acerra, C.; Aguacil, G.; Anastasiadis, A.; Atakan, K.; Azzara, R.M.; Bard, P.-Y.; Basili, R.; Bertrand, E.; Bettig, B.; Blarel, F.; et al. Guidelines for the Implementation of the H/V Spectral Ratio Technique on Ambient Vibrations—Measurements, Processing and Interpretation, SESAME European Research Project WP12—Deliverable D23.12, European Commission—Research General Directorate Project No. EVG1-CT-2000-00026 SESAME. December 2004. Available online: https://sesame.geopsy.org/Papers/HV_User_Guidelines.pdf (accessed on 31 December 2025).

41. Studio Geotecnico Italiano. Relazione Illustrativa—STUDIO DI MICROZONAZIONE SISMICA DI I LIVELLO—COMUNE DI VERONA. 2017. Available online: https://moodle2.units.it/pluginfile.php/563787/mod_resource/content/1/10_Liv.2-San%20Pietro%20di%20Feletto-Veneto.pdf (accessed on 31 December 2025).
42. Hibbit, Karlsson and Sorensen. *ABAQUS Theory and User's Manuals 2018*; Hibbit, Karlsson and Sorensen: Pawtucket, RI, USA, 2018.